

Compression and Free Expansion of Single DNA Molecules in Nanochannels

Christian Hermann Reccius,* John Thomas Mannion, Joshua David Cross, and H. G. Craighead

School of Applied and Engineering Physics, Cornell University, Ithaca, New York 14853, USA

(Received 10 August 2005; published 21 December 2005)

We investigated compression and ensuing expansion of long DNA molecules confined in nanochannels. Transverse confinement of DNA molecules in the nanofluidic channels leads to elongation of their unconstrained equilibrium configuration. The extended molecules were compressed by electrophoretically driving them into porelike constrictions inside the nanochannels. When the electric field was turned off, the DNA strands expanded. This expansion, the dynamics of which has not previously been observable in artificial systems, is explained by a model that is a variation of de Gennes's polymer model.

DOI: 10.1103/PhysRevLett.95.268101

PACS numbers: 87.14.Gg, 36.20.Ey, 87.15.-v

In the last decade biophysicists have utilized single molecule manipulation techniques to study the mechanical properties of DNA [1]. Among the more established methods are microscale techniques such as stretching [2], twisting [3], and unzipping DNA [4] by magnetic beads. Recent experiments have used nanostructures such as nanopores [5,6], nanopillar arrays [7], entropic traps [8], and nanochannels [9,10] to investigate DNA as well as the entropic forces, which dominate the molecular behavior at the nanoscale. Some of these new devices may even be candidates for replacing standard electrophoresis separation techniques [11–14].

Long DNA molecules such as λ -phage DNA form micron size spherical coils in free solution. Since these coils are difficult to resolve in detail with optical microscopy, previous quantitative studies have been restricted to investigating elongated DNA. However, many biophysical questions involve DNA compression, for instance, DNA packaging in chromatin or bacteriophage heads [15,16]. Confining DNA in nanochannels increases its equilibrium dimensions [9] and enables us to investigate this yet unreachable regime of compression and ensuing expansion.

In order to calculate the space taken up by a DNA molecule, it can be modeled as a polymer with N monomers corresponding to the base pairs, a monomer length a , a contour length $L = Na$, a persistence length b , and a width w . Describing the persistent chain as a flexible chain of rods with the Kuhn length $2b$ leads to the random walk radius $R_0 = (2Nab)^{1/2}$. But this result is too small because it neglects the expansion of the polymer due to volume exclusion [17]. This was first taken into account by Flory [18,19] and later generalized for persistent polymers by Schaefer *et al.*, who started with the free energy of a polymer as a function of its coil radius R [20]:

$$F_S(R) = \frac{1}{\beta} \left(\frac{3R^2}{2R_0^2} + \frac{vN^2}{2n^2R^3} \right), \quad (1)$$

with $\beta = (k_B T)^{-1}$, the number of monomers per rod $n = 2b/a$, and the excluded volume per rod v . The first term describes the entropic contribution from coil expansion, which leads to a contracting springlike force on the mole-

cule [21]. The second term, known from virial gas theory, covers self-avoidance and entropy of mixing effects, which lead to an expanding force on the polymer. Minimizing the free energy $F_S(R)$ leads to the well-known Flory radius $R_F = [a^2 v / (2n)]^{1/5} N^{3/5}$ of a polymer in solution. The excluded volume per rod is $v = \pi b^2 w$ according to Onsager [22].

We assume a polymer, which is elongated to the length l by confinement in a tube of diameter D . It can, according to de Gennes's "blob" model, be delineated as a series of $K = l/D$ nonpenetrating spheres with radius $D/2$ and N/K monomers [see Fig. 1(a)] [23]. Each sphere itself can be described by the Flory theory. The free energy becomes

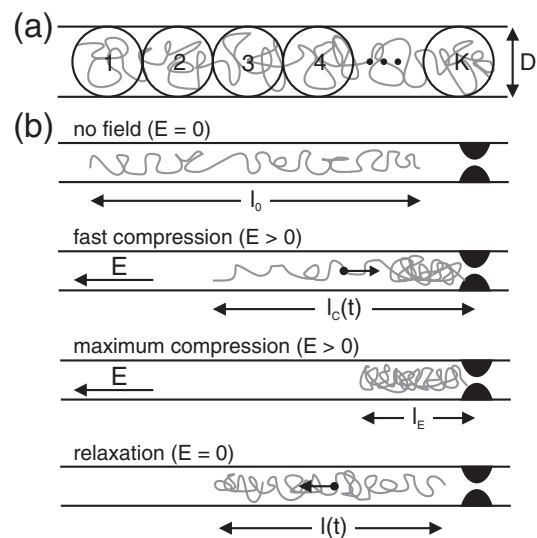


FIG. 1. (a) "Blob" model of confined DNA in a channel of diameter D describing the molecule as a series of K self-avoiding spheres. (b) Experimental stages of compressing a DNA molecule at a constriction. Without external force the DNA has the extended length l_0 . Under the influence of an electrical field E the strand initially compresses on the right and finally reaches the equilibrium length l_E . After turning off E the molecule expands back to the original length l_0 .

$$F(l) = KF_S(D/2) = \frac{1}{\beta} \left(\frac{4vN^2}{n^2D^2l} + \frac{3l^2}{8R_0^2} \right). \quad (2)$$

A similar scaling formula was obtained by Brochard-Wyart and Raphael for a polymer in a polymer melt [24]. A variation was proposed by Turban [25]. Minimizing the free energy leads to the unconstrained equilibrium length l_0 of a DNA strand in a channel:

$$l_0 = \left(\frac{16a^2v}{3D^2n} \right)^{1/3} N = \left(\frac{8\pi bw}{3D^2} \right)^{1/3} L. \quad (3)$$

This result is consistent with the de Gennes scaling theory [23].

We compress DNA in a constriction by an electrical field E until the equilibrium length l_E is reached [see Fig. 1(b)]. When the electrical field is turned off, the expansion of the molecule is only hindered by friction and therefore the force $f_{\text{exp}} = dF/dl$ can be related to the velocity of the center of mass of the molecule v and the viscous drag coefficient g by $f_{\text{exp}} = f_{\text{fric}} = g v$. Assuming that the right end of the molecule is not moving away from the constriction, we can set $v = (1/2)(dl/dt)$. As our channel diameters are of the order of the persistence length b , most of the hydrodynamic interactions between molecule segments are screened [26]. Thus the drag coefficient is assumed to be $g = \xi L = \xi N a$ with the friction coefficient per unit length ξ , which leads to a differential equation describing the free expansion of DNA:

$$\frac{1}{\beta} \left(-\frac{4N^2v}{n^2D^2l^2(t)} + \frac{3l(t)}{4R_0^2} \right) + \frac{1}{2} N a \xi \frac{dl(t)}{dt} = 0. \quad (4)$$

The solution for the initial condition $l(0) = l_E$ is

$$l(t) = \left[l_0^3 - (l_0^3 - l_E^3) \exp\left(-\frac{t}{\tau_d}\right) \right]^{1/3}, \quad (5)$$

with the time constant of molecule decompression

$$\tau_d = \frac{2}{9} \beta a^3 n \xi N^2 = \frac{4}{9} \beta \xi b L^2. \quad (6)$$

Note that this equation can be used to calculate the persistence length b if we know τ_d and the friction coefficient ξ of the channels.

The nanofluidic devices were fabricated by sealing a structured fused silica wafer with a thin cover wafer [27]. The mirror-polished wafers (Mark Optics, Santa Ana, CA) had thicknesses of 500 μm and 170 μm , respectively. An initial aluminum layer was made by electron-beam evaporation and covered by a poly(methyl-methacrylate) resist layer. The nanochannel part of the device was patterned with a JBX-9300FS electron-beam lithography system (JEOL, Peabody, MA) and transferred to the aluminum by reactive ion etching with a chlorine based process. Optical lithography and the same etching procedure were then used to define the microchannels in the aluminum mask layer. The whole pattern was transferred to the fused silica by a 200 nm deep reactive ion etch with CHF_3/O_2 .

The fluid reservoirs at the end of the microchannels were accessed from the backside of the substrate wafer by alumina powder blasting. Finally, the wafers were touch bonded and annealed at 1050 $^\circ\text{C}$. Constrictions were formed at random positions in the nanochannels by fluctuations of the aluminum mask width. An optical micrograph of the device is shown in Fig. 2. Note that the nanoscale constrictions are not visible.

Devices were filled with a buffer consisting of 200 mM tris-acetate and 5 mM EDTA ($5 \times \text{TAE}$, pH 8.3, Sigma, St. Louis, MO) with 5% (v/v) β -mercaptoethanol as an antiphotobleaching agent and 2.5% (w/w) poly(n -vinylpyrrolidone) (PVP, MW 10 000, Sigma) for preventing electro-osmotic flow as well as DNA sticking to the walls [28,29]. Platinum electrodes were placed in the channel reservoirs to enable electrophoretic drive of the DNA.

λ -phage DNA (12 $\mu\text{g}/\text{ml}$, New England Biolabs, Ipswich, MA) was stained with the intercalating dye YOYO-1 (Molecular Probes, Eugene, OR). The contour length of single λ -DNA (48.5 kbp) can be calculated from the base pair spacing of $a = 0.34$ nm to $L_\lambda = 16.5$ μm . Its persistence length is about $b = 51$ nm in physiological salt conditions [30]. However, recent studies have shown that the dye TOTO-1, which is a close derivative to YOYO-1, increases the contour length L_λ by 30%–35% at a dye to base pair ratio of 1:4 and the same is assumed to happen to the persistence length b [26,31]. Thus at our dye ratio of 1:5 L_λ is expected to rise by 23% to 20 μm and b to 63 nm. The individual molecules were observed with an IX70 inverted microscope (Olympus America, Melville, NY), which was equipped with a $100 \times /0.93$ NA oil immersion objective (Olympus) and illuminated by a 100 W mercury

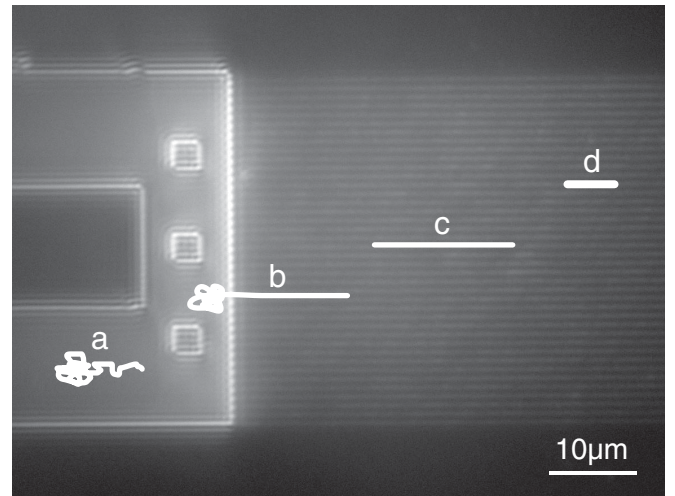


FIG. 2. Differential interference contrast micrograph of interface between micro- and nanochannel region. The nanochannels on the right have a width of 100 nm and a spacing of 900 nm. The three squares and the rectangle on the left are support pillars stabilizing the microchannel. Inserted in the picture are illustrations of DNA molecules entering the nanochannels from the microchannel (a)–(c) as well as a compressed strand (d).

arc lamp. An XF100 filter set (Omega Optical, Brattleboro, VT) was used for fluorescence imaging. The experiments were recorded with an ICCD-350F camera (Videoscope, Dulles, VA) connected to a DVD Recorder at a rate of 29.97 frames per second. The length of the molecules was automatically tracked by a MATLAB program (The Mathworks, Natick, MA).

Inside the nanochannels the majority of the investigated molecules, which we assume are λ -phage monomers, showed an extended length of $l_0 = 7 \pm 1 \mu\text{m}$. This result is slightly lower than the extended length of $8 \mu\text{m}$ measured for λ molecules in 100 nm channels [9]. We attribute the difference to our larger average channel diameter ($D = \sqrt{100 \text{ nm} \times 200 \text{ nm}} = 140 \text{ nm}$) [25]. Using Eq. (3) with a molecule width of $w = 2 \text{ nm}$, a dye corrected persistence length of $b = 63 \text{ nm}$, and a contour length of $L_\lambda = 20 \mu\text{m}$, we calculate $l_0 = 7.6 \mu\text{m}$, which is close to the measured value. Multiples of l_0 can be interpreted as multimers of λ -phage DNA [9].

The strands were compressed at the constrictions inside the nanochannels by an electric field of $E = 15.6 \text{ V/cm}$

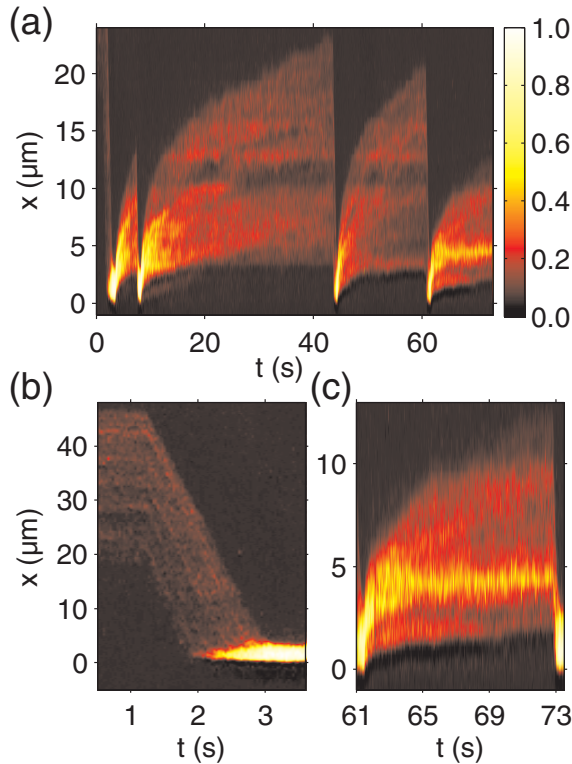


FIG. 3 (color). (a) Time course of four DNA compression and expansion experiments of four ligated λ molecules at a constriction (not visible) located at $x = 0$ by an electric field pointing upwards. The normalized intensity along the channel axis (x) is plotted as vertical lines versus the time t [10]. Each time the field was shut off the DNA expanded slowly upwards. (b) Zoom in on the first DNA compression with the electric field turned on at $t = 1.2 \text{ s}$ showing a continuous intensity built up at the constriction. (c) Zoom in on the fourth expansion showing a knot not unfolding at $x = 4\text{--}5 \mu\text{m}$.

calculated from device dimensions. The constrictions seem to have a negligible resistance as they did not affect the velocities of DNA molecules in the corresponding channels, which is probably due to a short length of the constrictions. Figure 3 shows repeated compression and free expansion of four ligated λ molecules as a color-coded intensity graph. It is clear that the first three expansions were faster than the last one. We attribute this to an incomplete unfolding in the latter case, evidence of which can be seen in Fig. 3(c). During the first few seconds of each expansion the whole molecule moved quickly away from the constriction. This may be due to a conical shape of the constrictions leading to an entropic repulsion [7]. Fluid backflow was not seen in any channel. The length variation during the first three expansions can be fit by Eq. (5) (see Fig. 4). The result is a decompression time constant of $\tau_d = 66.7 \pm 0.4 \text{ s}$. Equivalent experiments with concatemers consisting of one and two λ molecules led to $\tau_d = 13.1 \pm 0.3 \text{ s}$ and $\tau_d = 33.4 \pm 0.3 \text{ s}$, respectively.

According to Eq. (6) in order to calculate the persistence length b from the values of τ_d obtained from the fits, we have to determine the friction coefficient ξ of elongated DNA in our nanochannels. Thus DNA molecules with charge q and charge per unit length λ were driven by a constant electric field of $E = 15.6 \pm 0.1 \text{ V/cm}$ through the channels. As the electrical force $f_{\text{elec}} = qE = \lambda LE$ and the frictional force $f_{\text{fric}} = \xi L v$ are in force equilibrium, the friction coefficient can be calculated as $\xi = \lambda E / v$. Inserting $\lambda = 1.1 e_0 / \text{nm}$, which accounts for 61% shielded phosphodiester groups of the DNA backbone [32] at $\text{pH } 8.3$ and for a charge of $4e_0$ per YOYO-1 molecule, and a mean velocity of $v = 27.1 \pm 2.8 \mu\text{m/s}$ from 14 runs in defect free channels leads to a friction coefficient of

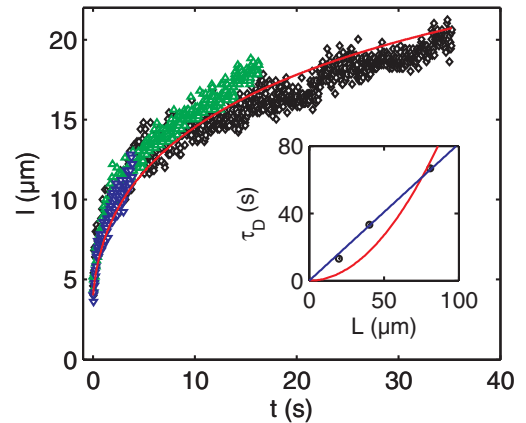


FIG. 4 (color). Extended length $l(t)$ of expanding DNA strand. The first three expansions out of four are fitted with Eq. (5) (red line) using the length of the uncompressed strand $l_0 = 27.8 \mu\text{m}$ and the compressed strand $l_E = 4.0 \mu\text{m}$ determined from Fig. 3(b). The resulting time constant of the fit is $\tau_d = 66.7 \pm 0.4 \text{ s}$. Inset: Fitted time constants τ_d versus contour length L for $1x$, $2x$, and $4x$ λ concatemers. Using Eq. (6) to fit the data (red line) leads to $b = 9.7 \pm 2.3 \text{ nm}$, although $\tau_D(L)$ is better described by a linear fit (blue line) with a slope of $0.91 \pm 0.03 \text{ s}/\mu\text{m}$.

$\xi = 10.3 \pm 1.1$ fNs/ μm^2 . This is a factor of 4 higher than the pure hydrodynamic friction coefficient $\xi = 2\pi\eta/\ln(D/w) = 2.8$ fNs/ μm^2 of a solid tube with diameter w inside another PVP-solution filled tube with diameter D using an estimated viscosity of $\eta = 1.8$ cPs. The calculated friction is a lower bound as it neglects DNA segment orientations as well as interactions with the channel walls.

Solving Eq. (6) for the persistence length b and using the determined ξ and τ_d , we calculate $b_{1x\lambda} = 28 \pm 3$ nm, $b_{2x\lambda} = 18 \pm 2$ nm, and $b_{4x\lambda} = 9 \pm 1$ nm for the different concatemers. The longer the DNA strand, the more b differs from the expected $b = 63$ nm. In addition, the inset of Fig. 4 shows that the measured τ_d depends approximately linearly on the contour length L instead of the quadratic behavior suggested by Eq. (6). Note that our calculation is highly depended on the estimated shielding of the DNA which could be influenced by cation enrichment at the channel walls. Higher shielding would lead to lower ξ and to a larger b .

The discrepancy between the three determined values for the persistence length may come from the fact that the longer the DNA strands, the higher the initial compression due to the electric field. Higher compression leads to sharper DNA bending. It is reasonable that DNA curved more sharply should be described by shorter rods in the virial gas interpretation. The smaller average rod size may also be caused by DNA kinking. This effect, known from DNA interactions with proteins or zinc ions [33,34], may here be induced by the compression force. It should also be noted that Schaefer's free energy model and de Gennes's blob model are the best available analytical model that account for volume-exclusion effects [1]. However, they do not account for the nonuniformity of the DNA strand during its initial compression by an electrical field. More sophisticated models such as the wormlike chain model could accommodate this nonuniformity very well, but would not account for volume-exclusion effects [35]. Variations of this model as well as numerical simulations may provide an even better framework through which to study this now experimentally reachable regime of single polymer compression.

In conclusion, we have with high precision optically investigated DNA relaxation from a compressed state. As far as the authors are aware, this is the first time that compressed DNA has been investigated quantitatively as opposed to stretched DNA [1]. We found that a variation of de Gennes's polymer model describes the experimental data. Future DNA compression studies may lead to a better understanding of the dependence of volume-exclusion effects on environmental parameters such as varying salt concentrations in physiological buffers. Devices containing nanochannels with nanoporelike constrictions could be used as tools for single polymer characterization and could even be combined with electrical measurements.

This work was supported by the Nanobiotechnology Center (NBTC). Device fabrication was performed in

part at the Cornell NanoScale Science and Technology Facility (CNF).

*Electronic address: hcf3@cornell.edu

- [1] T. R. Strick *et al.*, Rep. Prog. Phys. **66**, 1 (2003).
- [2] S. B. Smith, L. Finzi, and C. Bustamante, Science **258**, 1122 (1992).
- [3] T. R. Strick *et al.*, Science **271**, 1835 (1996).
- [4] B. Essevaz-Roulet, U. Bockelmann, and F. Heslot, Proc. Natl. Acad. Sci. U.S.A. **94**, 11 935 (1997).
- [5] J. Li *et al.*, Nature (London) **412**, 166 (2001).
- [6] J. Li *et al.*, Nat. Mater. **2**, 611 (2003).
- [7] S. W. P. Turner, M. Cabodi, and H. G. Craighead, Phys. Rev. Lett. **88**, 128103 (2002).
- [8] J. Han, S. W. Turner, and H. G. Craighead, Phys. Rev. Lett. **83**, 1688 (1999).
- [9] J. O. Tegenfeldt *et al.*, Proc. Natl. Acad. Sci. U.S.A. **101**, 10 979 (2004).
- [10] W. Reisner *et al.*, Phys. Rev. Lett. **94**, 196101 (2005).
- [11] J. Han and H. G. Craighead, Science **288**, 1026 (2000).
- [12] M. Cabodi, S. W. P. Turner, and H. G. Craighead, Anal. Chem. **74**, 5169 (2002).
- [13] M. Ueda *et al.*, J. Appl. Phys. **96**, 2937 (2004).
- [14] M. Streek *et al.*, Phys. Rev. E **71**, 011905 (2005).
- [15] S. C. Riemer and V. A. Bloomfield, Biopolymers **17**, 785 (1978).
- [16] D. E. Smith *et al.*, Nature (London) **413**, 748 (2001).
- [17] W. Kuhn, Kolloid Z. **68**, 2 (1934).
- [18] P. J. Flory, J. Chem. Phys. **17**, 303 (1949).
- [19] P. J. Flory, *Principles of Polymer Chemistry* (Cornell University Press, Ithaca, NY, 1953).
- [20] D. W. Schaefer, J. F. Joanny, and P. Pincus, Macromolecules **13**, 1280 (1980).
- [21] F. Bueche, *Physical Properties of Polymers* (Interscience, New York, NY, 1962).
- [22] L. Onsager, Ann. N.Y. Acad. Sci. **51**, 627 (1949).
- [23] P. G. de Gennes, *Scaling Concepts in Polymer Physics* (Cornell University Press, Ithaca, NY, 1979).
- [24] F. Brochard-Wyart and E. Raphael, Macromolecules **23**, 2276 (1990).
- [25] L. Turban, J. Phys. (Paris) **45**, 347 (1984).
- [26] O. B. Bakajin *et al.*, Phys. Rev. Lett. **80**, 2737 (1998).
- [27] S. M. Stavis, J. B. Edel, K. T. Samiee, and H. G. Craighead, Lab Chip **5**, 337 (2005).
- [28] Q. Gao and E. S. Yeung, Anal. Chem. **70**, 1382 (1998).
- [29] S. H. Kang, M. R. Shortreed, and E. S. Yeung, Anal. Chem. **73**, 1091 (2001).
- [30] C. Bouchiat *et al.*, Biophys. J. **76**, 409 (1999).
- [31] T. T. Perkins, D. E. Smith, R. G. Larson, and S. Chu, Science **268**, 83 (1995).
- [32] D. Stigter, Biophys. Chem. **101**, 447 (2002).
- [33] S. C. Schultz, G. C. Shields, and T. A. Steitz, Science **253**, 1001 (1991).
- [34] W. Han *et al.*, Proc. Natl. Acad. Sci. U.S.A. **94**, 10 565 (1997).
- [35] D. Stigter and C. Bustamante, Biophys. J. **75**, 1197 (1998).